OPEN

Oncogene (2017) **36**, 6839–6849

www.nature.com/onc

ORIGINAL ARTICLE

Identification of translationally controlled tumor protein in promotion of DNA homologous recombination repair in cancer cells by affinity proteomics

Y Li[1,6], H Sun[1,6], C Zhang[2,6], J Liu[1], H Zhang[1], F Fan[1], RA Everley[3], X Ning[1], Y Sun[1], J Hu[1], J Liu[2], J Zhang[2], W Ye[2], X Qiu[2], S Dai[4], B Liu[4], H Xu[5], S Fu[1], SP Gygi[3] and C Zhou[1]

Translationally controlled tumor protein (TCTP) has been implicated in the regulation of apoptosis, DNA repair and drug resistance. However, the underlying molecular mechanisms are poorly defined. To better understand the molecular mechanisms underlying TCTP involved in cellular processes, we performed an affinity purification-based proteomic profiling to identify proteins interacting with TCTP in human cervical cancer HeLa cells. We found that a group of proteins involved in DNA repair are enriched in the potential TCTP interactome. Silencing TCTP by short hairpin RNA in breast carcinoma MCF-7 cells leads to the declined repair efficiency for DNA double-strand breaks on the GFP-Pem1 reporter gene by homologous recombination, the persistent activation and the prolonged retention of γH2AX and Rad51 foci following ionizing radiation. Reciprocal immunoprecipitations indicated that TCTP forms complexes with Rad51 *in vivo*, and the stability maintenance of Rad51 requires TCTP in MCF-7 cells under normal cell culture conditions. Moreover, inactivation of TCTP by sertraline treatment enhances UVC irradiation-induced apoptosis in MCF-7 cells, and causes sensitization to DNA-damaging drug etoposide and DNA repair inhibitor olaparib. Thus, we have identified an important role of TCTP in promoting DNA double-stand break repair via facilitating DNA homologous recombination processes and highlighted the great potential of TCTP as a drug target to enhance conventional chemotherapy for cancer patients with high levels of TCTP expression.

Oncogene (2017) **36,** 6839–6849; doi:10.1038/onc.2017.289; published online 28 August 2017

INTRODUCTION

Genomes of all organisms must endure constant DNA damage challenges that arise from endogenous DNA replication errors and environmental insults including chemical carcinogens, viral infection, ionizing radiation (IR) and ultraviolet (UV) irradiation. To combat these genotoxic stresses and maintain genome stability, cells have evolved a signaling cascade termed DNA damage response along with a variety of DNA repair processes dedicated to counteracting various types of DNA damage lesions.[1,2] DNA damage response senses different types of DNA damage and coordinates various cellular responses including activation of transcription, cell cycle arrest, apoptosis and initiation of DNA repair processes.[3] DNA damage lesions caused by genotoxic exposure include base modifications, interstrand crossing, single-strand breaks and double-strand breaks. Of these, double-strand breaks are the most severe DNA damage lesions, and they are repaired by either non-homologous end joining (NHEJ) or homologous recombination (HR) or both repair pathways.[4] NHEJ is a template free, and thus error prone, process that occurs primarily in the G1 phase of cell cycle. DNA-PKcs (DNA-dependent protein kinase, catalytic subunits), Ku70/Ku80, LIG4/ERCC4, LIG3, LIG1[5–7] and so on, are the major components of NHEJ and its alternative pathways. By contrast, HR requires a homologous DNA sequence as a template, which is an error-free repair process that mainly occurs in the S and G2–M phases.[8] The key participants of HR repair processes include MRE11-Rad50-NBS1 complex, ATM, ATR, H2AX, RPA1, CtIP, BRCA1, BRCA2, Rad51, and its paralogs such as Rad51B, Rad51C[9–14] and so on. Failure of repairing those DNA damage lesions and/or defects of DNA damage response signaling and repair machinery often lead to genome instability including increased gene mutations, chromosome rearrangements as well as gain or loss of entire chromosomes, which are perhaps the main culprit of human abnormal development, immunodeficiency diseases and even tumorigenesis.

Translationally controlled tumor protein (TCTP, also called TPT1, p23 or fortilin) is an evolutionary conserved small protein that does not share significant homology with any known proteins or domains.[11,15–17] It has been demonstrated TCTP involves in many cellular processes. For example, TCTP was upregulated in response to oxidative stress, heat shock and DNA damage.[15,18,19] Furthermore, TCTP also stimulates cell survival by interacting with antiapoptotic Bcl-xL and suppressing Bax-mediated proapoptotic pathways.[20,21] Several recent studies have shown that TCTP participates in HR repair via association with ATM[22] and in NHEJ repair processes through its interaction with DNA-PKcs.[19] In addition, TCTP was shown to promote the ubiquitin-mediated degradation of TP53,[23,24] a tumor suppressor that plays a critical role in orchestrating activation of cell cycle checkpoints,

[1]The Laboratory of Medical Genetics, Harbin Medical University, Harbin, China; [2]The 2nd Affiliated Hospital, Harbin Medical University, Harbin, China; [3]Department of Cell Biology, Harvard Medical School, Boston, MA, USA; [4]The Tumor Hospital, Harbin Medical University, Harbin, China and [5]Department of Clinical Laboratory, The First Affiliated Hospital, Dalian Medical University, Dalian, China. Correspondence: Professor C Zhou, The Laboratory of Medical Genetics, Harbin Medical University, 157 Baojian Road, Nangang District, Heilongjiang, Harbin 150081, China.
E-mail: Chunshuizhou@163.com
[6]These authors contributed equally to this work.
Received 27 February 2017; revised 9 June 2017; accepted 13 July 2017; published online 28 August 2017

subsequent DNA repair processes and induction of apoptosis and senescence.[25,26]

To better understand the molecular mechanisms underlying TCTP involved in cellular processes, we used an immunoprecipitation-based proteomic approach to identify the proteins interacting with TCTP in human cervical cancer HeLa cells. We found that a group of proteins involved in HR repair were enriched in the TCTP interactome. We further demonstrated that Rad51, a critical player in HR repair, is associated with TCTP, and a high level of TCTP is required for efficient HR repair in breast carcinoma MCF-7 cells and for the stability maintenance of Rad51 in cells under normal conditions. We also provided evidence that the chemical inactivation of TCTP can sensitize cancer cells to DNA-damaging agents.

RESULTS

Identification of TCTP interactome in HeLa cells

To better understand how TCTP participates in various cellular processes, we aimed to identify proteins interacting with TCTP in human cells. We established a HeLa cell line (with a low level of endogenous TCTP expression) stably expressing 3 × Flag-TCTP driven by mammalian expression vector pcDNA3.1. Whole-cell lysates were prepared from the 3 × Flag-TCTP-expressing cells or control cells transformed with an empty vector. M2 antibodies against Flag peptide were used for immunoprecipitation in above cell lysates. The resulting bound proteins were resolved on 15% sodium dodecyl sulfate–polyacrylamide gel electrophoresis (SDS–PAGE) gels, stained with Coomassie blue and each lane in the gel was cut into six slices. Peptides were generated via in-gel trypsin digestion and subjected to liquid chromatography tandem-mass spectrometry (LC-MS/MS). An outline of our profiling approach is shown in Figures 1a–c. By comparison with proteins identified in the control immunoprecipitation (IP), we removed many obvious contaminated proteins including keratin and most abundant nonspecific binding proteins such as ribosomal proteins and method-biased proteins binding to magnetic protein A beads. Eventually, a total of 145 candidates potentially interacting with TCTP in HeLa cells were obtained (Supplementary Table S1).

TCTP involves in DNA damage signaling and repair

We submitted these candidate proteins to PANTHER biological process tool for gene ontology analysis.[27] We found that apoptosis (4%), ubiquitination (7%), response to stimuli (5%) and so on are the major functional categories among these TCTP-interacting candidates (Figure 2a). Most strikingly, a group of proteins under the DNA replication and repair category were significantly enriched (10%) in the TCTP potential interactome (Figure 2a). These proteins including RAD51B, a key player in HR repair; BRAT1, a binding partner of BRCA1; BCCIP, a protein associating with BRCA2; MRE11 and NBS1, components of MRE11-Rad50-NBS1 DNA damage sensing complex; PIKK kinase ATR and DNA-PKcs, and so on, are well known for their roles in HR- and NHEJ-mediated double-strand DNA repair (Figure 2b). We also used GeneMANIA program to identify networks among these DNA repair-related candidates,[28] and discovered several important DNA repair modules such as HR repair, nucleotide excision repair, replication factor C (RFC), COP9/signalosome/CSN-Cul4A-DDB and NHEJ (Figures 2c–g); these well-defined functional modules are crucial for repair of DNA double-strand breaks and ultraviolet irradiation-caused photoproducts. To further verify the link between TCTP and DNA repair pathway, we treated HeLa cells with 300 ng/ml neocarzinostatin (NCS, a radiomimetic drug causing DNA double-strand breaks), harvested the treated cells at various time points post NCS withdrawl from the medium and determined the endogenous TCTP protein level by western blot. We found that the TCTP level transiently increased upon NCS treatment, its level peaked at 2 h time point post NCS treatment and gradually dropped back to its original level (Supplementary Figure S1), consistent with previous findings that DNA-damaging agents cisplatin and etoposide are able to increase TCTP stability.[11,29] Furthermore, immunostaining of 3 × Flag-TCTP in NCS-treated cells (at 2 h time point post recovery) indicated that TCTP is a predominantly cytoplasmic protein. Following NCS treatment, there was a slight increase of overall signal of 3 × Flag-TCTP in cells, but neither prominent nuclear relocalization of TCTP nor nuclear TCTP foci formation was observed, except that some cytoplasmic foci of TCTP occurred in both untreated and NCS-treated cells independent of DNA damage (Supplementary Figure S2a). Subcellular fractionation experiments revealed that there is a weak signal of 3 × Flag-TCTP appeared in the nuclear fraction at 2 h time point post NCS treatment (Supplementary Figure S2b), which is consistent with a previous finding reported by Zhang *et al*.[19] Therefore, despite that TCTP responds to DNA damage by a small increase of its abundance, it is more likely for TCTP to involve in the DNA repair process as a regulatory player rather than as a candidate repair enzyme accumulated on the sites of DNA damage. The fact of no nuclear TCTP foci formation upon DNA damage has further strengthened our above assumption.

Deficiency of TCTP impairs HR repair efficiency in cancer cells

Given the fact that a group of HR proteins occurred in our TCTP interactome, we would like to determine whether TCTP involves in the HR repair of DNA double-strand breaks. In this regard, we worked on the breast carcinoma MCF-7 cells because of a high level of endogenous TCTP expression in these cells. We integrated GFP-PEM1 HR reporter gene cassettes into MCF-7 cells with TCTP silenced by short hairpin RNA (shRNA) (hereafter referred to as shTCTP-1, for western blot confirmation of TCTP-knockdown cell lines, see Supplementary Figure S3) or with a control shRNA against firefly luciferase mRNA (hereafter referred to as shFF2), and expressed restriction enzyme I-Sce I in the two cell lines by transient plasmid transfection. Upon I-Sce I cleavage on the GFP-Pem1 gene, the HR-mediated gene conversion will reconstitute the full fluorescent GFP gene[30] (for detailed repair processes see Supplementary Figure S4). Thus, we measured HR efficiency by counting GFP-positive cells upon I-Sce I induction. At 24 h time point after induction of I-Sce I, the average percentage of GFP-positive cells in shFF2 or shTCTP-1 is 3.24 ± 0.06% and 0.64 ± 0.39%, respectively, and at 48 h time point post induction, the percentage is increased to 4.99 ± 1.21% and 1.06 ± 0.30%, respectively (Figures 3a–c). Obviously, there are fewer GFP cells in shTCTP-1 cells compared with shFF2 cells at both 24 and 48 h time points after I-Sce I induction ($P < 0.01$, at 48 h). The lower percentage of GFP-positive cells in the TCTP silencing cells suggested that TCTP is required for efficient HR repair in MCF-7 cells. To confirm our observed changes of HR repair efficiency are related to the TCTP expression level, not an effect of shRNA off-target, we ectopically overexpressed shRNA-resistant TCTP in the above shTCTP-1 cells (for the exact mutation sites of TCTP shRNA-resistant gene see Materials and methods section). We found that the percentages of GFP-positive cells in this rescued cell line are similar to the shFF2 cells at both 24 and 48 h post I-Sce I induction while the GFP-positive cells remain low in the empty vector-transformed shTCTP-1 cells, indicating that the improved HR repair is due to the restoration of high level expression of TCTP in the TCTP-knockdown cells (Figures 3d and e).

Furthermore, we used immunostaining to assess the foci formation of γH2AX and Rad51, two key markers for DNA damage signaling and HR repair processes, in both shFF2 and shTCTP-1 cells irradiated with 10 Gy of γ-ray. At 2 h time point post IR irradiation, the average foci number of Rad51 per shFF2 and shTCTP-1 cell was 23.43 ± 10.15 and 22.73 ± 7.05, respectively. After 12 h of recovery, the foci number of Rad51 in shFF2 cells

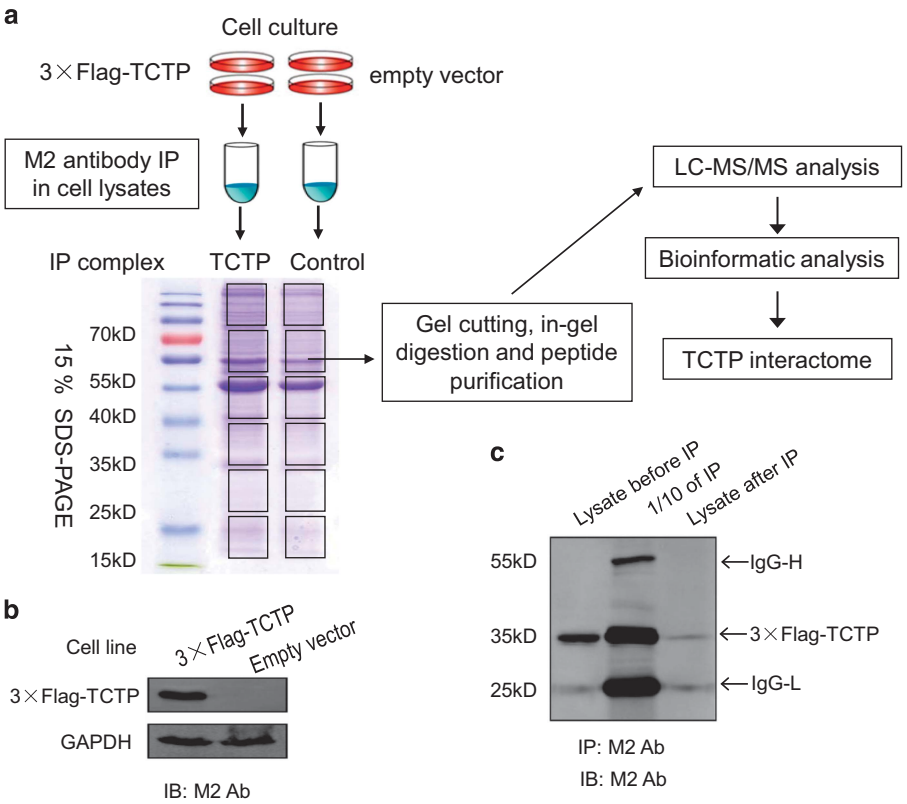

Figure 1. Proteomic identification of TCTP interactome by immunoprecipitation (IP). (**a**) Schematic of the workflow of profiling of TCTP-interacting proteins by IP combined with LC-MS/MS. Cell lysates were prepared from HeLa cells stably expressing 3 × Flag-TCTP or control cells transformed with the empty vector. The M2 antibody-coupled magnetic beads were used for IP. The resulting bound proteins were resolved on a 15% SDS–PAGE gel, the gel was stained with Coomassie blue and cut into slices. Peptides were extracted from in-gel trypsin digestion and subjected to LC-MS/MS. (**b**) Western blot (WB) verification of 3 × Flag-TCTP overexpression in HeLa cells. M2 antibody was used at 1:1000 of dilution, and GAPDH was as a loading control. (**c**) The efficiency of anti-Flag antibody-mediated TCTP IP. M2 antibody was used for both IP and WB. Bound proteins were resolved on 15% SDS–PAGE gels. IgG-L and IgG-H are the light and heavy chains of M2 antibody.

dropped to 9.98 ± 2.90 (Figures 3f and g). By contrast, the number and signal intensity of Rad51 foci in shTCTP-1 cells remained high (20.64 ± 6.37) in comparison with shFF2 cells ($P < 0.01$). In addition, the foci formation of γH2AX behaved in a manner similar to Rad51 foci (Figures 3h and i). Therefore, the persistent activation of γH2AX and prolonged retention of Rad51 foci in shTCTP-1 cells suggested that the efficiency of HR repair is impaired upon TCTP silencing.

Association of Rad51 with TCTP *in vivo* and decreased stability of Rad51 upon TCTP knockdown

How TCTP affects HR repair in MCF-7 cells is unclear; we checked the interaction between TCTP and a couple of candidates such as Rad51, Mre11 and BRAT1 from our screen by antibody-mediated reciprocal immunoprecipitation in MCF-7 cells. The reciprocal IP results indeed confirm the association of Rad51 with TCTP (Figure 4a). However, when we mixed GST-Rad51 protein with 6xHis-TCTP protein purified from transformed *Escherichia coli* expressing Rad51 or TCTP fusion protein and performed GST pull-down assay, we failed to observe the obvious direct binding activity between each other, except that some weak nonspecific binding signal related to the glutathione magnetic beads (Figure 4b). Thus, we conclude that Rad51 might be indirectly associated with TCTP in MCF-7 cells. Several previous studies indicated that TCTP may regulate the protein stability of TP53 and MDM2.[23] Therefore, we checked the half-life of Rad51 protein, a key player in HR repair processes, in MCF-7 cells with shTCTP-1 or shFF2 expression. We treated these cells with 50 μg/ml of cycloheximide (CHX), harvested at various time points and determined TCTP protein level by western blotting. We found that the average half-life of Rad51 in shFF2 cells is 45.3 ± 7.5 min, whereas the average half-life of Rad51 in shTCTP-1 cells decreases to 30.2 ± 6.3 min ($P < 0.05$) (Figures 4c and d). The decreased half-life of Rad51 indicates that Rad51 becomes less stable upon knockdown of TCTP. As a result, the short half-life of Rad51 may lead to impaired HR repair capacity in TCTP-deficient cells. However, following 10 Gy of IR, the Rad51 protein was stabilized (Figure 4c, lower panel). Interestingly, this kind of stabilization seems out of the TCTP control. Taken together, our data suggested that a high level of TCTP is required for maintaining the stability of Rad51 in MCF-7 cells.

Inactivation of TCTP by sertraline causes enhanced apoptosis induced by DNA damage and increased sensitization to etoposide and olaparib

TCTP has been implicated in the regulation of apoptosis,[15] and a number of chemical compounds such as antimalaria drug dihydroartemisinin, antihistaminic agents and antidepressant drug sertraline have been shown to be able to inhibit the expression of TCTP in human and rodent cells and tissues.[31–33] Therefore, we want to determine whether inactivation of TCTP by sertraline could sensitize MCF-7 cells to DNA-damaging agents' treatment. We cultured MCF-7 cells in the presence of sertraline and determined the optimal sertraline using a concentration of

2.5 μM by cell viability assay (MTT (3-(4,5-dimethylthiazol-2-yl)-2,5-diphenyltetrazolium bromide assay, data not shown). Under such a concentration, the cultured cells display both normal morphology and proliferation, whereas the TCTP protein level in the treated cells decreases significantly after 24 h of sertraline treatment (Figure 5a). Moreover, at 24 h time point following 2.5 μM sertraline treatment, we subjected the treated MCF-7 cells to 20 J/m^2 UVC irradiation. After 24 h of recovery, the cells were

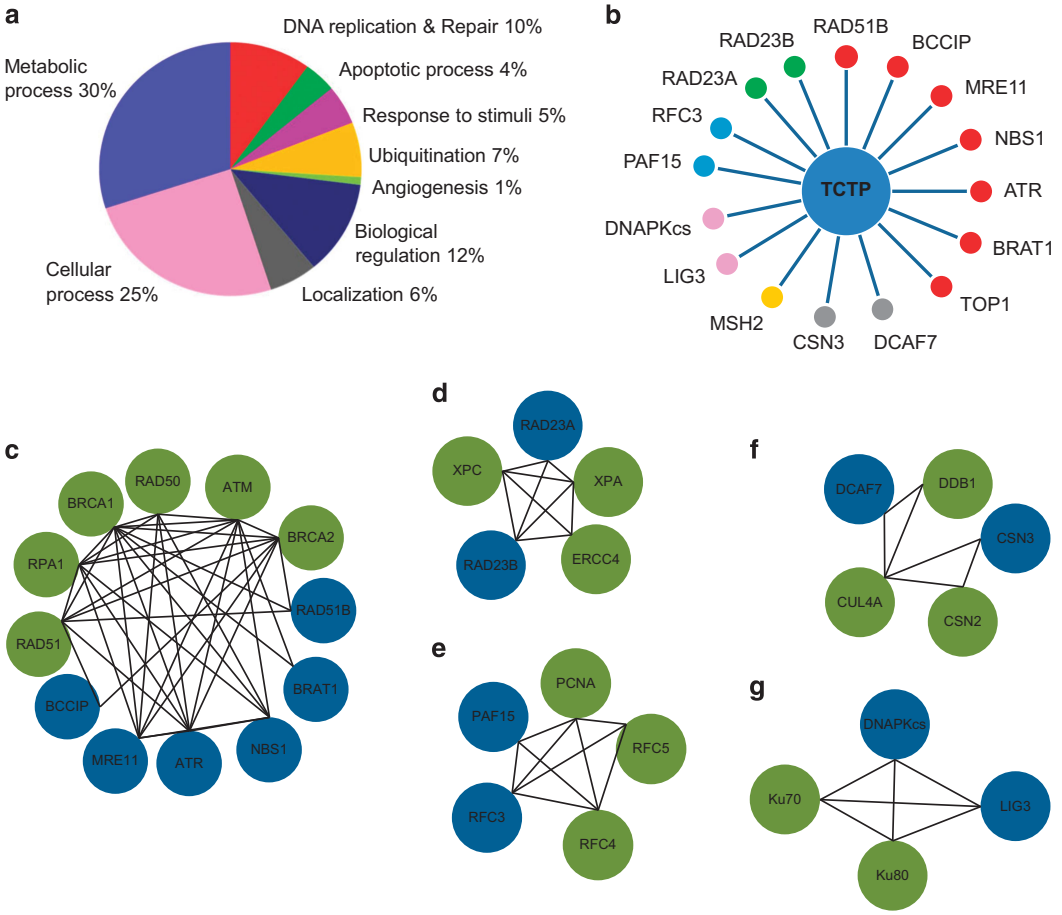

Figure 2. Gene ontology (GO) analysis of potential TCTP interactome. (**a**) Classification of biological processes of TCTP interactome by PANTHER Classification System. A total of 145 candidates were analyzed. (**b**) A group of proteins involving in DNA replication and repair are enriched in the TCTP interactome. (**c**–**g**) Network modeling of candidates in (**b**) was analyzed by using GeneMANIA program, and the selected functional modules with at least more than two identified candidates are shown as follows: (**c**) DNA HR repair module; (**d**) nucleotide excision repair (NER) module; (**e**) replication factor C (RFC) module; (**f**) CSN-DDB module; (**g**) NHEJ module. In each module, solid lines indicate bilateral interactions, proteins identified in our screen are marked in blue and other related proteins are in green.

Figure 3. Knockdown of TCTP in MCF-7 cells impairs the HR repair efficiency. (**a** and **b**) shFF2 and shTCTP-1 cells integrated with GFP-PEM1 cassettes were transiently co-transfected with I-Sce I and orange fluorescence protein (OFP) expression vectors. GFP-positive cells were observed under fluorescence microscopy and measured by flow cytometry at the indicated time points following I-Sce I induction. The representative images of GFP-expressing cells in the two cell lines under fluorescence microscopy with magnification of ×100 are shown in (**a**). The representative flow cytometry data are shown in (**b**). (**c**) The quantitative summary of flow cytometry data. Data are presented as mean ± s.d. from at least three independent I-Sce I induction experiments and normalized to OFP-expressing cells for transfection efficiency control. An error bar represents s.d. $^{**}P < 0.01$ indicates a significant difference by Student's *t*-test. (**d**) Ectopic expression of shRNA-resistant TCTP in TCTP-knockdown cells restores HR repair efficiency. pcDNA3.1(−) 3 × Flag-TCTP-shRNA-resistant or the empty vectors were transfected into shTCTP-1 cells integrated with GFP-PEM1 reporter gene. Stable expression cell lines were established after 200 μg/ml hygromycin B selection. The average GFP-positive cells were counted by fluorescence-assisted cell sorting (FACS) after the indicated times of I-Sce I induction in the shRNA-resistant TCTP expression or empty vector control cells. $^{**}P < 0.01$ indicates a significant difference by Student's *t*-test. (**e**) Overexpression confirmation of 3 × Flag-TCTP-shRNA resistant in MCF-7 shTCTP-1 cells by western blotting. (**f** and **h**) Knockdown of TCTP prolonged the retention time of the foci of endogenous Rad51 and γH2AX. shFF2 and shTCTP-1 cells were irradiated with 10 Gy of γ-ray, and recovered for the indicated times; cells were fixed, permeabilized and processed for immunofluorescence staining using antibodies against Rad51 and γH2AX. Nuclei were counterstained with 4′,6-diamidino-2-phenylindole (DAPI). The representative foci formation images at indicated time points were shown in (**f**) and (**h**) (×1000). (**g** and **i**) Graphs in (**g**) and (**i**) represent quantitative summaries of Rad51 and γH2AX foci, respectively. A total of 100 cells were counted for foci formation, the average foci number per cell was determined from at least three independent IR experiments and data are presented as mean ± s.d. Error bars represent s.d. $^{**}P < 0.01$ indicates a significant difference by Student's *t*-test.

submitted to Annexin V-mediated fluorescence-assisted cell sorting. We found that there were more apoptotic cells in sertraline-treated cells upon UVC irradiation (9.05 ± 0.36%) than the cells without sertraline treatment (4.54 ± 0.32%, $P < 0.001$) (Figures 5b and c). Apoptosis is a common consequence induced by extensive DNA damage from endogenous repair defects and/or exogenous insults. Therefore, to demonstrate that the enhanced apoptosis by sertraline treatment upon UV irradiation is relevant to DNA repair impairment caused by inactivation of TCTP, we examined whether sertraline could have synergistic effects on the colony formation ability of MCF-7 cells exposed to the DNA-damaging drug etoposide. Cells were treated with a single dose of 0.5 μM etoposide for 1 h on day 1, and then cultured in fresh medium containing 2.5 μM sertraline for 7 days. The average cologenic survival rate in the group of etoposide combined with sertraline treatment was significantly decreased compared with etoposide treatment alone (13.1 ± 5.7% vs 35.5 ± 7.28%, $P < 0.05$) (Figures 5d and e), indicating sertraline treatment can sensitize cancer cells to DNA-damaging drugs. To further prove the relevance of sertraline treatment to DNA repair capacity, we

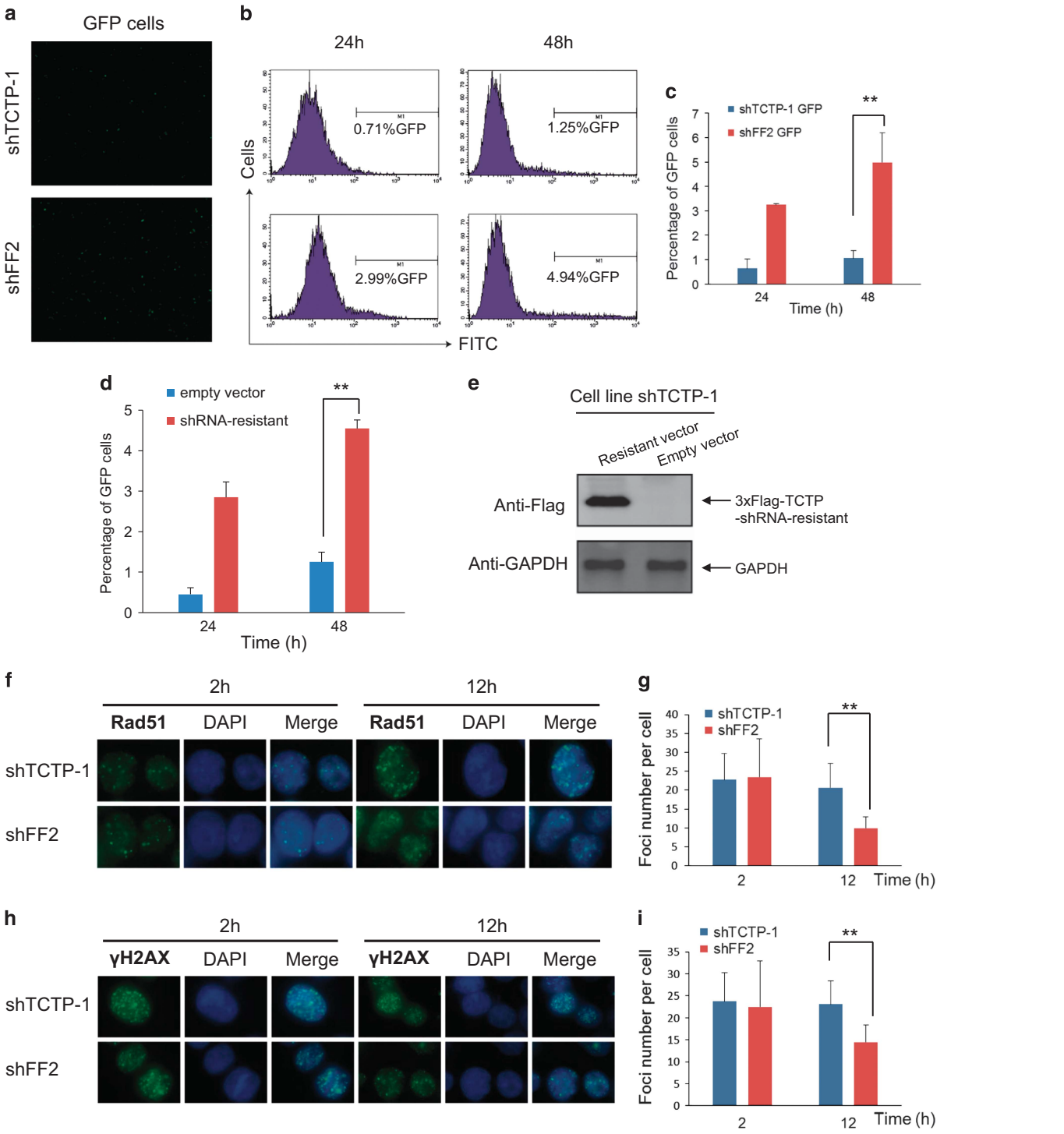

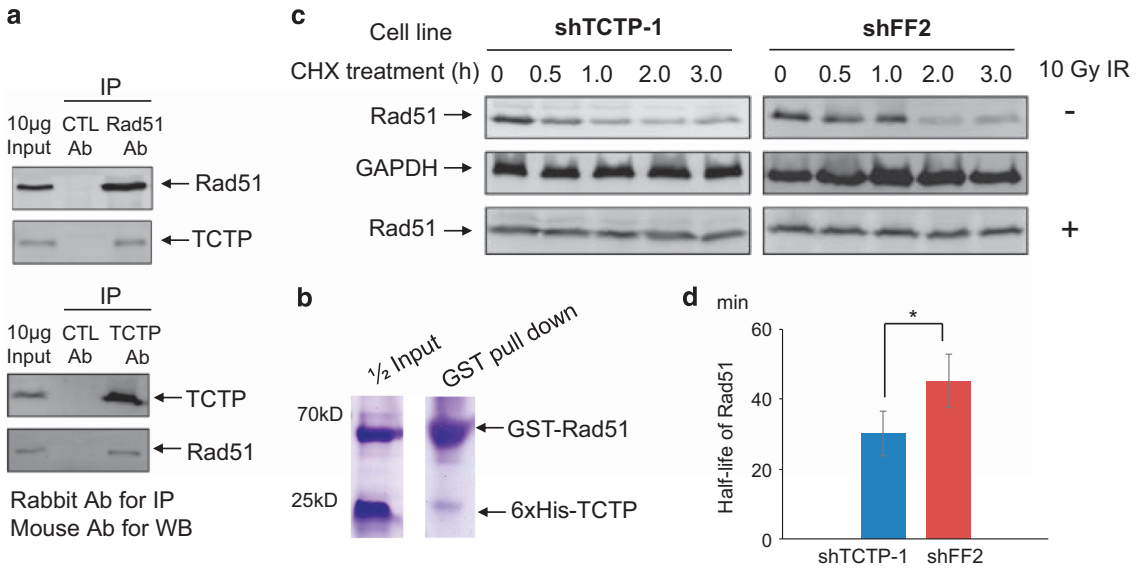

Figure 4. Association of Rad51 with TCTP *in vivo* and knockdown of TCTP leads to decreased stability of Rad51 in MCF-7 cells. (**a**) Verification of the association of Rad51 with TCTP in cells. One microgram of antibodies against Rad51 or TCTP were used for each reciprocal immunoprecipitation in a total of 1 mg of MCF-7 cell lysates, and the precipitated proteins were resolved on SDS–PAGE gel and probed with indicated antibodies. (**b**) No direct binding activity detected between purified Rad51 and TCTP. GST-Rad51 and 6×His-TCTP proteins were purified from expression vector-transformed BL21 *E. coli* by using glutathione or Ni-NTA magnetic beads, 20 μg of each protein were mixed together and subjected to GST pull down, proteins were resolved on SDS–PAGE gel and stained with Coomassie blue. (**c**) The representative western blot images of Rad51 protein stability. TCTP knockdown of MCF-7 cells (shTCTP-1) or control cells (shFF2) at log phase were seeded into 6 cm plates, after one day of culture, 50 μg/ml of CHX was added into each plates (for DNA damage exposure, cells were irradiated with 10 Gy of IR before CHX treatment) and cells were harvested at the indicated time points. A total of 40 μg cell lysate of each sample were loaded and resolved on 12% SDS–PAGE gels, and an antibody against Rad51 was used for probing the endogenous Rad51. (**d**) The half-life of Rad51 in TCTP-knockdown cells is decreased. The signal intensity of Rad51 in (**c**) was determined by densitometry in comparison with the signal at time zero without CHX treatment, and normalized to GAPDH. The half-life of Rad51 was calculated based on at least three independent CHX treatments and plotted in (**d**), and data are presented as mean ± s.d. (min). An error bar represents s.d. *$P < 0.05$ indicates a significant difference by Student's *t*-test.

tested whether sertraline could enhance the growth inhibition of olaparib,[34] a specific inhibitor for poly (ADP-ribose) polymerase 1 and 2, which prevent the formation of DNA double-strand breaks,[35,36] on MCF-7 cells in another setting of cologenic assays. As shown in Figure 5f, sertraline treatment indeed greatly sensitized MCF-7 cells to olaparib inhibition by a little more than twofold increase of olaparib sensitivity. Furthermore, we examined the endogenously arising γH2AX foci formation in the cells from the cologenic assay because poly (ADP-ribose) polymerase inhibitors can induce spontaneous double-strand breaks and γH2AX foci formation.[36] Compared with olaparib treatment alone, the treatment of sertraline in combination with olaparib greatly increased the mean number of endogenously arising γH2AX foci per positive nucleus (from 4.54 ± 2.75 to 10.62 ± 3.98, $P < 0.05$) (Figure 5g) and the average percentage of foci-positive cells (from 7.5 to 36.3%) (Figure 5h), indicating that sertraline treatment indeed can exacerbate the DNA double-strand breaks triggered by olaparib.

Finally, we examined the cytotoxicity kinetics of etoposide treatment on MCF-7 cells upon knockdown of endogenous TCTP by measuring cell survival and proliferation; we found that knockdown of TCTP also led to the enhanced growth inhibition of etoposide, in particular, at the high dose exposure of etoposide compared with shFF2 control cells, whereas the reintroduction of a Flag-tagged shRNA-resistant TCTP in the TCTP-knockdown cell line almost restored its etoposide resistance to a level similar to that displayed in the shFF2 cell line (Supplementary Figure S5). Thus, the DNA damage sensitization caused by knockdown of TCTP is in good agreement with what we have observed in the inactivation by sertraline treatment. Taken together, our data indicate that there is an intrinsic DNA repair defect underlying the inactivation of TCTP by sertraline and uphold the great potential for TCTP as a new therapeutic target for cancer targeting therapy in the clinic.

DISCUSSION

To determine the composition of highly dynamic protein complexes in cells is a great challenge. Affinity purification coupled with comparative and/or quantitative proteomics has been proven a powerful approach to identify protein interaction networks at the proteome level.[37–39] Based on this strategy, we discovered 145 proteins (TCTP itself not included) with the potential of interacting with TCTP in HeLa cells. A close examination found only a few known TCTP interactors such as DNA-PKcs and histone family members appear in our list,[19] whereas numerous other TCTP-interacting proteins including ATM, MDM2, Mcl-1 (myeloid cell leukemia-1), Bcl-xL, PLK1, tubulin, Hsp27 and Na-K-ATPase[17,19,20,40–43] are missing from our list. We consider the following reasons may account for such a discrepancy between our TCTP interactome and previous findings. First, some TCTP protein complexes may be only formed and stabilized under a given circumstance such as apoptosis or genotoxic stress, whereas our affinity purification was performed in cells cultured under normal conditions. Second, low abundance and/or low stoichiometry of certain interacting proteins may impede them to be identified during mass spectrometry. Third, the dynamic nature of the association of protein kinases such as PLK1 and ATM with TCTP may cause the failure of capturing these transient interactors by immunoprecipitation.

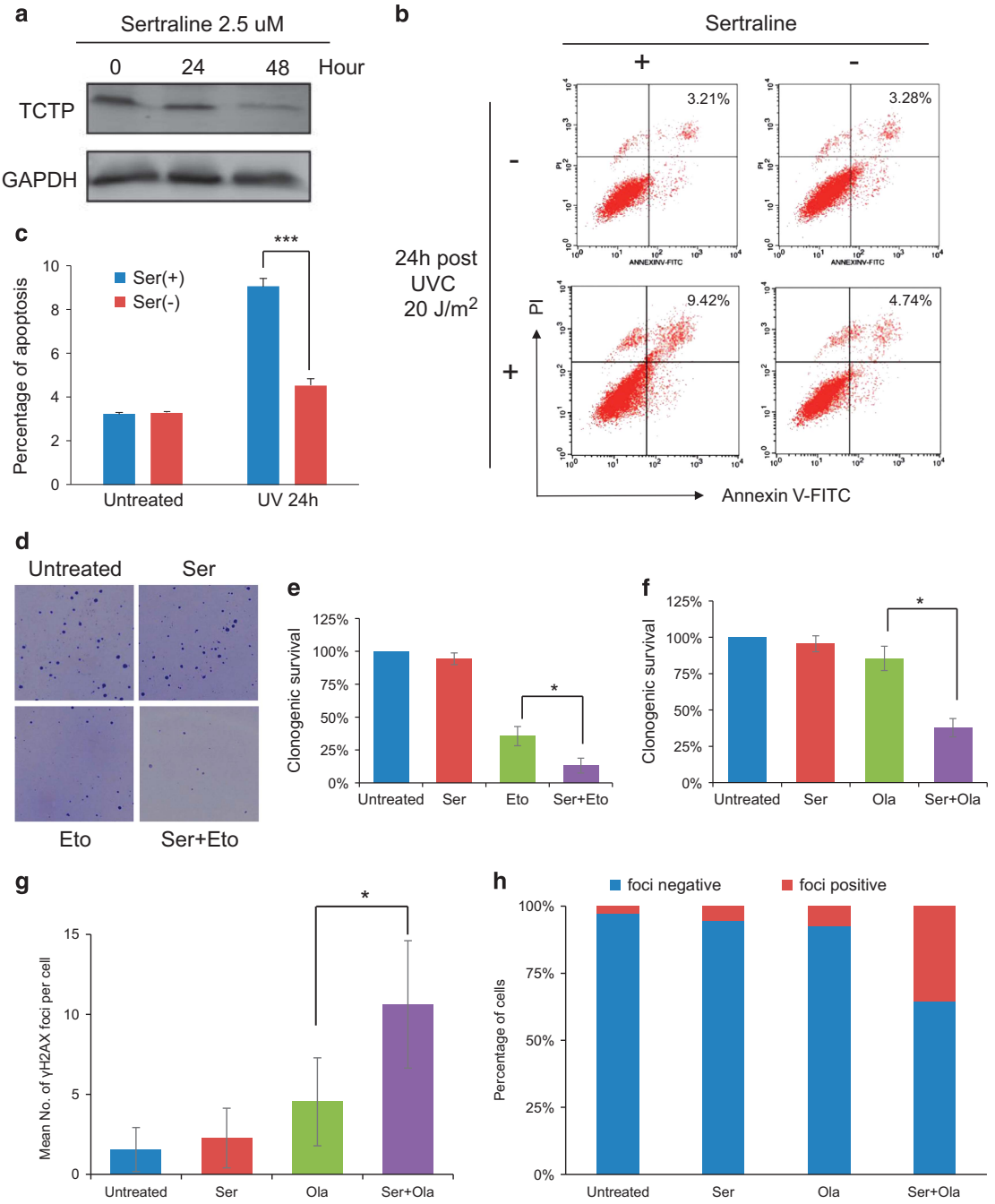

Figure 5. Inactivation of TCTP by sertraline results in increased apoptosis upon DNA damage and sensitization to etoposide and olaparib. (**a**) Western blot confirmation of the inhibition of TCTP expression by sertraline treatment (2.5 μM) in MCF-7 cells at the indicated time points. (**b**) MCF-7 cells were treated with sertraline (2.5 μM) for 24 h and exposed to 20 J/m^2 UVC. Cells were harvested at 24 h time point after UVC. The proportions of apoptotic cells were determined by Annexin V-mediated flow cytometry. (**c**) The quantitative summary of UVC-induced apoptotic cells from three independent sertraline treatment experiments. ***$P < 0.001$ indicates a significant difference by Student's *t*-test. (**d** and **e**) Sensitization of etoposide by sertraline. MCF-7 cells treated with 0.5 μM etoposide for 1 h alone or in combination with continuous presence of 2.5 μM sertraline for 7 days. Representative cologenic assay images were shown in (**d**) and the average number of colonies (⩾50 cells) from three independent assays were normalized to the untreated control and plotted in (**e**). Error bars represent s.d. *$P < 0.05$ indicates a significant difference between the indicated two groups by Student's *t*-test. (**f**) Sensitization of poly (ADP-ribose) polymerase (PARP) inhibitor olaparib by sertraline. Cologenic assay were performed in the continuous presence of 0.5 μM olaparib alone or in combination with 2.5 μM sertraline during the assay. The average survival rate of each group from three independent assays was graphed in (**f**). *$P < 0.05$ indicates the significant difference by Student's *t*-test. (**g** and **h**) The endogenously arising γH2AX foci were increased significantly upon combination treatment. The cells from (**f**) were fixed with paraformaldehyde and stained with anti-γH2AX antibodies. The foci were counted under fluorescence microscopy, the mean number of foci per positive nucleus and the average percentage of γH2AX-positive cells of each treatment were plotted in (**g**) and (**h**), respectively. *$P < 0.05$ indicates the significant difference by Student's *t*-test.

On the other hand, our TCTP affinity purification profiling may have revealed many more new potential TCTP interactors. For example, MRE11 and NBS1, components of MRE11-Rad50-NBS1 complex for DNA damage sensing and activation of ATM kinase, were identified as candidates associated with TCTP. In addition to DNA damage response signaling, proteins involved in double-strand break repair such as BRCA1-interacting protein BRAT1[44,45] and BRCA2-associated protein BCCIP[46] showed up in our TCTP interactome, hinting the potential role of TCTP in the maintenance of genome stability in HeLa cells. In fact, TCTP has been implicated in both NHEJ and HR repair.[19,22] The nuclear translocation of Ku70 and Ku80, two crucial players of NHEJ, requires a certain level of TCTP following IR in human skin AG1522 cells.[19] ATM, a key regulator for HR repair, is also known for its interaction with TCTP in the control of genome stability and organ development of *Drosophila*.[22] Moreover, a number of TCTP-associated proteins identified in our profiling, including RAD51B, ATR, MRE11, NBS1, BRAT1, BCCIP, DNA-PKcs and LIG3, are more or less involved in either HR or NHEJ, or even both pathways. One fact that needs to be pointed out is that we failed to observe the direct binding activity between GST-Rad51 and 6xHis-TCTP proteins purified from transformed *E. coli* expressing Rad51 or TCTP, although we were able to confirm the association of Rad51 with TCTP in MCF-7 cells by reciprocal immunoprecipitation. Hence, we assume that the link between HR repair processes and TCTP may be indirect. Indeed, the fact that no obvious changes of subcellular localization of TCTP upon NCS treatment and no nuclear TCTP foci formation following double-strand breaks further strengthen our assumption (Supplementary Figure S2). Furthermore, the indirect link between TCTP and HR repair is consolidated by the mechanisms of the TCTP-mediated regulation of proapoptotic protein Bax and tumor suppressor TP53.[21,23]

We found that TCTP is required for maintaining the stability of Rad51 in MCF-7 cells, and how TCTP affects the stability of Rad51 is unclear so far. Some hints may arise from previously published observations. First, the binding of TCTP to MDM2 inhibits the autoubiquitination of MDM2 and increases MDM2 level.[23] Second, Mcl-1 protein could bind to TCTP and cause stabilization of TCTP probably via inhibition of ubiquitin-proteasome pathway.[40] Consistent with these observations, a number of proteins related to ubiquitin degradation pathway indeed appeared in our TCTP interactome, suggesting that TCTP might involve in ubiquitin-mediated degradation of proteins including Rad51. Alternatively, TCTP may act as a molecular chaperone for protecting RAD51 from degradation. TCTP itself is protected by chaperone protein Hsp27 from misfolding and ubiquitin-proteasome degradation.[43,47] Thus, downregulation of TCTP via gene silencing or Hsp27 dysfunction would render RAD51 more susceptible to misfolding and protein degradation.[18] In this regard, more vigorous investigations are needed to elucidate the underlying mechanisms.

We have demonstrated that antidepressant chemical drugs such as sertraline can sensitize MCF-7 cells to DNA damage treatment. However, the mechanism by which sertraline suppresses cell resistance to DNA damage has not been fully understood. Previous studies suggest that the direct binding of sertraline to TCTP protein would inhibit the association of TCTP with MDM2;[23] as a consequence, the upregulation of MDM2 autoubiquitination leads to the accumulation of TP53, which renders the cells more prone to apoptosis upon genotoxic stress. In addition, a low level of TCTP may result in the derepression of dimerization of Bax, which is required for its proapoptotic activity in cells. Alternatively, we found that inhibition of TCTP by sertraline-sensitizing cells to DNA-damaging drug etoposide and poly (ADP-ribose) polymerase inhibitor olaparib probably is the consequence of the impairment of HR repair, because a certain level of TCTP is required for efficient HR processes. Towards this point, the promotion of HR repair by TCTP is unlikely the only factor accounting for cell resistance to DNA-damaging agents. Consistent with a previous finding,[19] the DNA ligase LIG3 and PIKK kinase DNA-dependent protein kinase complexes revealed in our TCTP interactome strongly suggest that the TCTP-mediated NHEJ pathway should also contribute to the repair of DNA double-strand breaks other than HR repair.

The fact that high levels of TCTP are associated with malignancy progression and chemoresistance makes TCTP an intriguing target for chemotherapy to human cancer treatment.[15,23,31] It has been shown that silencing TCTP expression by small interfering RNA induces caspase-dependent cell death and increases the efficacy of chemotherapy in castration-resistant LNCaP cells.[47] Hence, it is plausible for exploring a chemical TCTP inhibitor in combination with conventional chemotherapeutics to improve the effectiveness of conventional chemotherapy for a group of human cancer patients with high levels of TCTP expression. Our observations of sensitization of DNA-damaging drug etoposide and poly (ADP-ribose) polymerase inhibitor olaparib by inactivation of TCTP with sertraline treatment also offer more clinical relevance to radiation therapy or chemotherapy for cancer treatment. In addition to our *in vitro* results, more *in vivo* experiments such as testing in mouse tumor models need to be done before any clinical trials. Given the fact that sertraline is a widely used antidepression drug and its pharmacology is largely known,[48,49] it would be plausible for us to explore the application of sertraline or its derivatives as a new class of TCTP targeting sensitizers for human cancer treatment in the future.

In summary, by using affinity purification-based proteomic profiling, we have identified a role of TCTP in the regulation of DNA repair, in particular, the HR repair. The unanticipated role of TCTP in HR processes not only sheds new insight into the molecular mechanism underlying HR repair but also highlights the great potential for exploiting chemical inhibitors against TCTP in combination with conventional chemotherapy for the better treatment of human cancers in the clinic.

MATERIALS AND METHODS

Cell lines and DNA damage treatment

Human cancer cell lines HeLa and MCF-7 were purchased from ATCC (Manassas, VA, USA). Cells were grown under standard tissue culture conditions (37 °C, 5% CO_2) in RPMI-1640 (HeLa) containing 10% fetal bovine serum or DMEM (MCF-7) containing 10% fetal bovine serum. For DNA damage treatment, cells were subjected to 300 ng/ml NCS or 10 Gy of ionizing radiation (γ-ray, generated from a Cobalt-60 source at the second affiliated hospital of Harbin Medical University, Harbin, China) or 20 J/m^2 UVC irradiation (UV Crosslinker; Hoefer Inc., Holliston, MA, USA).

Antibodies and chemical reagents

All chemicals including NCS, neomycin (G418), puromycin, sertraline, CHX, MS grade water, acetonitrile and formic acid were purchased from Sigma-Aldrich (St Louis, MO, USA). Porcine sequencing grade modified trypsin was bought from Promega (Fitchburg, WI, USA). Etoposide was purchased from Yeasen Biotechnology Inc. (Shanghai, China). Olaparib was purchased from Meilunbio Inc. (Dalian, China). Antibodies against TCTP (Cell Signaling Technology, Danvers, MA, USA, no. 7178; Santa Cruz, Dallas, TX, USA, sc-100763), glyceraldehyde-3-phosphate dehydrogenase (GAPDH) (Cell Signaling Technology, no. 5174), phospho-histone H2AX (Ser139) (Cell Signaling Technology, no. 3014), Rad51 (Calbiochem, Billerica, MA, USA, PC130; Merck Millipore, Billerica, MA, USA, 05-525), Flag M2 antibody (Sigma-Aldrich, F1804), anti-mouse secondary antibody (Rockland, Limerick, PA, USA, no. PV-9000), anti-rabbit secondary antibody (Rockland, no. 611-130-122), magnetic protein A beads (Invitrogen, Carlsbad, CA, USA) and so on were purchased from the indicated companies, respectively. For western blotting, antibodies were used at a dilution of 1:1000, and for immunofluorescence staining, antibodies were used at 1:400.

Immunoprecipitation and LC-MS/MS analysis

A total of 4×10^7 HeLa cells expressing 3 × Flag-TCTP or an empty vector at log phase were harvested by trypsin digestion and centrifugation. The cells were washed with phosphate-buffered saline (PBS), and lysed with 2 ml RIPA buffer containing 50 mM Tris (pH 7.4), 150 mM NaCl, 1 mM EDTA, 0.25% sodium deoxycholate, proteinase inhibitor cocktail (Roche, Basel, Switzerland) for 20 min at 4 °C. The lysate mixture was subjected to sonication to completely disrupt cells. Lysates were clarified by centrifugation at 14 000 r.p.m. for 30 min at 4 °C . Twenty micrograms of mouse anti-Flag antibody and 100 µl of magnetic protein A beads were added to 2 ml of TCTP or control lysates containing 100 mg of total proteins. Immunoprecipitation was performed for 4 h at 4 °C with gentle rotation. Bound immunocomplexes on beads were washed with RIPA buffer for three times and an aliquot of 10 µl of bead slurry was taken for western blotting. The remaining bound proteins on the beads were eluted by boiling in 2 × SDS–PAGE gel sample loading buffer, and resolved on a 15% SDS–PAGE gel and stained with Coomassie blue. Gel slices were cut and digested with trypsin at 37 °C overnight. Peptides were extracted with 50% acetonitrile, 0.1% formic acid and dried in a speed vacuum. Each peptide sample was desalted by stage tip[50] and analyzed by LC-MS/MS on a LTQ-Orbitrap Velos mass spectrometer (Thermo Fisher Scientific, Carlsbad, CA, USA). MS/MS spectra were searched via the SEQUEST algorithm against a composite database containing the Uniprot_Human database (46, 441 sequences) and its reversed complement. Search parameters are allowed for dynamic modifications of oxidation on Met or deamidation on Asn or Gln and up to two missed cleavages and maximum modifications $\leqslant 3$ per peptide. Matches were filtered with common parameters (mass tolerance $\leqslant 0.5$ Da, XCorr $\geqslant 2.0$) to a peptide false discovery rate $< 1\%$.[51]

Cloning and plasmid construction for gene expression or silencing

For TCTP cloning, total RNA was extracted from HeLa cells using TRIzol reagent. cDNAs were synthesized by the qScript cDNA Super-Mix Kit (Invitrogen). The coding region of TCTP (GenBank Accession No. NM_003295) was amplified from above cDNAs by using the following gene-specific primers: TCTP-F, 5′-GCATCTCGAGATGATTATCTACCGGGA-3′ and TCTP-R, 5′-GCATGAATTCCTAAAGATGTATTCCCCAATTC-3′ and cloned into pcDNA3.1 (−) 3 × Flag vector (Invitrogen) through *Xho*I/*Eco*RI restriction sites. The correct construct was confirmed by DNA sequencing. GV102 plasmid expressing shRNA for TCTP silencing were purchased from Genechem (Shanghai, China) containing the following TCTP targeting sequence: 5′-ACATCCTTGCTAATTTCAA-3′ (shTCTP-1) and 5′-AGGAAAC AAGTTTCACAAA-3′ (shTCTP-2), or 5′-CGCCTGAAGTCTCTGATTA-3′ (shFF2) against the firefly luciferase gene as negative shRNA control for gene silencing. The TCTP expression or silencing plasmids were transfected with Lipofectamine 2000 transfection reagent (Invitrogen) into the desired cells and transfected cell lines were selected in the presence of 200 µg/ml hygromycin B or 2.0 µg/ml puromycin (Sigma-Aldrich), and individual cell clones were confirmed by western blotting with antibodies against the target proteins. For bacterial expression of GST-Rad51 fusion protein, the coding region of Rad51 (GenBank Accession No. NM_002875.4) was amplified from above cDNAs by using the following gene-specific primers: Rad51-F, 5′-AATGGATCCATGGCAATG-CAGATGCAGCTTG-3′ and Rad51-R, 5′-TTAGCGGCCGCTCAGTCTTTGGCATCTCCCAC-3′ and cloned into pET-41a (+) (Novagen, Billerica, MA, USA) via *Bam*HI and *Not*I sites. For bacterial expression of 6xHis-TCTP, the following primers were used for amplification of TCTP: TCTP-His-F, 5′-GCATCTCGAGCATGATTATCTACCGGGA-3′ and TCTP-His-R, 5′-ACTGGAATTCCTAAAGATGTATTCCCCAATTC-3′, and the resulting TCTP gene was cloned into pBad/His A (Invitrogen) via *Xho*I and *Eco*RI sites.

Site-directed mutagenesis

For generating shRNA-resistant TCTP mutant gene, the following primer pairs containing desired mutations were used for site-directed mutagenesis of TCTP, shTCTP-1-resistant primer-F: 5′-CAGAACAAATCAAGCATCTA GCACTGGACTTTAAAAACTACCAGTTCTT-3′ and shTCTP-1 resistant primer-R: 5′-AAGAACTGGTAGTTTTTAAAGTCCAGTGCTAGATGCTT-GATTTGTTCTG-3′. pcDNA3.1 (−) 3 × Flag-TCTP plasmid was used as template for high fidelity PCR and digested with *Dpn*I restriction enzyme after PCR, the newly synthesized TCTP mutant expression plasmid DNA was transformed into *E. coli*, the desired TCTP shRNA-resistant gene was verified by DNA sequencing.

Affinity purification of fusion protein expressed from *E. coli*

pET-41a (+) vector expressing GST-Rad51 or pBad/His A vector expressing 6xHis-TCTP (Invitrogen) was transformed into BL21 *E. coli*, the transformed bacteria were cultured in LB medium until its optical density 600 nm reached to 1.0. Isopropylthiogalactoside or L-arabinose (Sigma-Aldrich) was added into the culture at a concentration of 0.2 mM and the desired expression of protein was inducted for 8 h at 30 °C. The bacteria were harvested by centrifugation and lysed by sonication. GST-Rad51 or 6xHis-TCTP protein was affinity purified by using glutathione or Ni-NTA magnetic beads (Thermo Fisher Scientific). Bound proteins were eluted with solution containing glutathione or imidazole and dialyzed against PBS buffer as the methods described in the user manual provided by the manufacturer.

Immunofluorescence for DNA damage foci formation

Cells were cultured on coverslips. After the desired DNA damage treatment, cells were fixed in 4% (wt/vol) paraformaldehyde for 10 min at room temperature, permeabilized in 0.2% Triton X-100 in PBS for 10 min, blocked with 4% (wt/vol) bovine serum albumin and incubated with the primary antibodies (Rad51 or γ-H2AX) overnight and followed by incubating with secondary goat-anti-rabbit antibodies conjugated with FITC (Alexa Fluor 488) or Texas Red (Alexa Fluor 594) labeling (Invitrogen) for 1 h at room temperature. Coverslips were mounted in 4′,6-diamidino-2-phenylindole (DAPI) containing media (Vectashield, Burlingame, CA, USA). Signals were visualized using a Leica DM500 B fluorescence confocal microscope (Wetzler, Germany). DNA damage foci were analyzed by using the Image J software (NIH, Bethesda, MD, USA).

Homologous recombination repair assay

GFP-Pem1 reporter and HA-I-Sce I expression vectors were kindly provided by Dr Vera Gorbunova (University of Rochester, Rochester, NY, USA). GFP-Pem1 cassettes were stably integrated into the desired cell lines. The resulting cell lines were transiently co-transfected with HA-I-Sce I expression and orange fluorescence protein expression vectors (Life Technologies, Carlsbad, CA, USA), cells were harvest at various time points post I-Sce I induction, GFP-positive cells were detected by fluorescence-assisted cell sorting (BD Biosciences, San Jose, CA, USA) and the percentage of GFP cells was normalized to orange fluorescence protein expression cells for transfection efficiency control. Expression of GFP was also monitored and recorded under fluorescence microscopy (Nikon, Eclipse Ti-S, Minato, Tokyo, Japan) at various time points.

MTT assay for cell proliferation and cytotoxicity

Cells were plated at a density of 5000 cells per well in 96-well plates at 37 °C in 5% CO_2 atmosphere. After 24 h of culture, the medium in the wells was replaced with fresh medium containing 2.5 µM sertraline (or 0.25, 0.5, 1.0 µM etoposide) for another 24 h (1 h for etoposide, after drug removal another 72 h culture) incubation. Then, the medium was removed and methanethiosulfonate assay was performed according to the manual provided by the manufacturer (Invitrogen). Absorbance at 495 nm is directly proportional to the number of viable cells in culture. Inhibition of cell growth was calculated as (optical density 495 nm of untreated − optical density 495 nm of treated)/optical density 495 nm of untreated. All measurements were performed in triplicate. The morphological phenotypes of sertraline-treated cells were also examined under light microscopy.

Colony formation assay

Trypsinized cells were seeded into 10 cm plates (250 cells per plate) and cultured overnight. For etoposide sensitization experiment, etoposide were added into each well at a final concentration of 0.5 µM for 1 h on day 1, drugs were removed and followed by a continuous 2.5 µM sertraline treatment for 7 days with medium change every other day. For olaparib sensitization experiment, 0.5 µM olaparib alone or in combination with 2.5 µM sertraline were added into cells on the following day 1, and continuously presented in the medium with medium change every other day for 7 days. Survival cells were stained with Giemsa and colonies with more than 50 cells were counted manually. The survival rates were calculated as average colonies versus seeding cell numbers and normalized to colonies formed from the untreated groups.

Flow cytometry

For apoptotic cells detection, the desired cells with appropriate treatments were harvested by trypsin digestion and washed in cold PBS buffer, and then cells were incubated with Annexin V-FITC conjugates in PBS buffer containing 1 mg/ml propidium iodide and 0.1 mg/ml RNase A. After 30 min incubation in dark, samples were subjected to flow cytometry (BD Biosciences). For GFP expression detection, the desired cells were trypsinized and resuspended in PBS solution and subjected to fluorescence-assisted cell sorting.

Protein half-life measurement

Cells at log phase were seeded into 6 cm plates. After one day of culture, 50 μg/ml of CHX was added into each plate, and cells were harvested at 30 min interval for a total of 3 h period of time course. The whole-cell lysates were prepared by adding 100 μl of 2 × SDS loading buffer to each plate, and the lysates were collected and subjected to sonication. A total of 40 μg cell lysate of each sample were loaded and resolved on 12% SDS–PAGE gels, an antibody against Rad51 was used for probing endogenous Rad51. The western blot signals were quantified by densitometry scanning and Image J analysis. The GAPDH signal was also detected and used for normalization. The calculation of the average Rad51 half-life was based on the signal versus time curve generated from at least three independent CHX treatments.

Bioinformatic analysis

Gene annotation was obtained from the Uniprot_Human database, Gene Ontology analysis was performed by the Panther Classification System.[27] A GeneMANIA program was used for network modeling and functional module discovery.[28]

Statistical analysis

For statistical evaluation, data are expressed as mean ± standard deviation. Statistical differences for comparisons of TCTP expression level and cell growth were determined by Student's *T*-test. The changes of apoptosis and GFP cells and foci numbers were examined by the one-way analysis of variance analysis. All analyses were performed using SPSS for Windows 13.0 software (SPSS Inc., Chicago, IL, USA). $P < 0.05$ (two tailed) was considered statistically significant.

CONFLICT OF INTEREST

The authors declare no conflict of interest.

ACKNOWLEDGEMENTS

We thank Professor Vera Gorbunova of the University of Rochester for providing the GFP-Pem1 reporter plasmid and CMV-HA-I-Sce I expression plasmid for detection of HR. We also thank Drs Bo Zhai, Willi Haas of SPG lab for their assistance and advice, and Dr Noah Dephoure's critical comments on manuscript writing. YL, HS, JL, HZ and CZ are supported by Grant No. 81272582 from the National Natural Science Foundation of China, HX is supported by Grant No. 31600662 from the National Natural Science Foundation of China. RAE and SPG are supported by National Institutes of Health, USA.

REFERENCES

1 Zhou BB, Elledge SJ. The DNA damage response: putting checkpoints in perspective. *Nature* 2000; **408**: 433–439.
2 Jackson SP, Bartek J. The DNA-damage response in human biology and disease. *Nature* 2009; **461**: 1071–1078.
3 Ciccia A, Elledge SJ. The DNA damage response: making it safe to play with knives. *Mol Cell* 2010; **40**: 179–204.
4 Lieber MR. The mechanism of human nonhomologous DNA end joining. *J Biol Chem* 2008; **283**: 1–5.
5 Lu G, Duan J, Shu S, Wang X, Gao L, Guo J *et al.* Ligase I and ligase III mediate the DNA double-strand break ligation in alternative end-joining. *Proc Natl Acad Sci USA* 2016; **113**: 1256–1260.
6 Lieber MR. The mechanism of double-strand DNA break repair by the nonhomologous DNA end-joining pathway. *Annu Rev Biochem* 2010; **79**: 181–211.
7 Simsek D, Brunet E, Wong SY, Katyal S, Gao Y, McKinnon PJ *et al.* DNA ligase III promotes alternative nonhomologous end-joining during chromosomal translocation formation. *PLoS Genet* 2011; **7**: e1002080.
8 San Filippo J, Sung P, Klein H. Mechanism of eukaryotic homologous recombination. *Annu Rev Biochem* 2008; **77**: 229–257.
9 Lee JH, Paull TT. ATM activation by DNA double-strand breaks through the Mre11-Rad50-Nbs1 complex. *Science* 2005; **308**: 551–554.
10 You Z, Chahwan C, Bailis J, Hunter T, Russell P. ATM activation and its recruitment to damaged DNA require binding to the C terminus of Nbs1. *Mol Cell Biol* 2005; **25**: 5363–5379.
11 Li F, Zhang D, Fujise K. Characterization of fortilin, a novel antiapoptotic protein. *J Biol Chem* 2001; **276**: 47542–47549.
12 Jazayeri A, Falck J, Lukas C, Bartek J, Smith GC, Lukas J *et al.* ATM- and cell cycle-dependent regulation of ATR in response to DNA double-strand breaks. *Nat Cell Biol* 2006; **8**: 37–45.
13 Sartori AA, Lukas C, Coates J, Mistrik M, Fu S, Bartek J *et al.* Human CtIP promotes DNA end resection. *Nature* 2007; **450**: 509–514.
14 Suwaki N, Klare K, Tarsounas M. RAD51 paralogs: roles in DNA damage signalling, recombinational repair and tumorigenesis. *Semin Cell Dev Biol* 2011; **22**: 898–905.
15 Acunzo J, Baylot V, So A, Rocchi P. TCTP as therapeutic target in cancers. *Cancer Treat Rev* 2014; **40**: 760–769.
16 Amson R, Pece S, Marine JC, Di Fiore PP, Telerman A. TPT1/ TCTP-regulated pathways in phenotypic reprogramming. *Trends Cell Biol* 2013; **23**: 37–46.
17 Gachet Y, Tournier S, Lee M, Lazaris-Karatzas A, Poulton T, Bommer UA. The growth-related, translationally controlled protein P23 has properties of a tubulin binding protein and associates transiently with microtubules during the cell cycle. *J Cell Sci* 1999; **112**(Part 8): 1257–1271.
18 Gnanasekar M, Dakshinamoorthy G, Ramaswamy K. Translationally controlled tumor protein is a novel heat shock protein with chaperone-like activity. *Biochem Biophys Res Commun* 2009; **386**: 333–337.
19 Zhang J, de Toledo SM, Pandey BN, Guo G, Pain D, Li H *et al.* Role of the translationally controlled tumor protein in DNA damage sensing and repair. *Proc Natl Acad Sci USA* 2012; **109**: E926–E933.
20 Yang Y, Yang F, Xiong Z, Yan Y, Wang X, Nishino M *et al.* An N-terminal region of translationally controlled tumor protein is required for its antiapoptotic activity. *Oncogene* 2005; **24**: 4778–4788.
21 Susini L, Besse S, Duflaut D, Lespagnol A, Beekman C, Fiucci G *et al.* TCTP protects from apoptotic cell death by antagonizing bax function. *Cell Death Differ* 2008; **15**: 1211–1220.
22 Hong ST, Choi KW. TCTP directly regulates ATM activity to control genome stability and organ development in *Drosophila melanogaster*. *Nat Commun* 2013; **4**: 2986.
23 Amson R, Pece S, Lespagnol A, Vyas R, Mazzarol G, Tosoni D *et al.* Reciprocal repression between P53 and TCTP. *Nat Med* 2012; **18**: 91–99.
24 Rho SB, Lee JH, Park MS, Byun HJ, Kang S, Seo SS *et al.* Anti-apoptotic protein TCTP controls the stability of the tumor suppressor p53. *FEBS Lett* 2011; **585**: 29–35.
25 Batchelor E, Loewer A, Lahav G. The ups and downs of p53: understanding protein dynamics in single cells. *Nat Rev Cancer* 2009; **9**: 371–377.
26 Li T, Liu X, Jiang L, Manfredi J, Zha S, Gu W. Loss of p53-mediated cell-cycle arrest, senescence and apoptosis promotes genomic instability and premature aging. *Oncotarget* 2016; **7**: 11838–11849.
27 Hurov KE, Cotta-Ramusino C, Elledge SJ. A genetic screen identifies the Triple T complex required for DNA damage signaling and ATM and ATR stability. *Genes Dev* 2010; **24**: 1939–1950.
28 Tkach JM, Yimit A, Lee AY, Riffle M, Costanzo M, Jaschob D *et al.* Dissecting DNA damage response pathways by analysing protein localization and abundance changes during DNA replication stress. *Nat Cell Biol* 2012; **14**: 966–976.
29 Sinha P, Kohl S, Fischer J, Hutter G, Kern M, Kottgen E *et al.* Identification of novel proteins associated with the development of chemoresistance in malignant melanoma using two-dimensional electrophoresis. *Electrophoresis* 2000; **21**: 3048–3057.
30 Mao Z, Tian X, Van Meter M, Ke Z, Gorbunova V, Seluanov A. Sirtuin 6 (SIRT6) rescues the decline of homologous recombination repair during replicative senescence. *Proc Natl Acad Sci USA* 2012; **109**: 11800–11805.
31 Tuynder M, Fiucci G, Prieur S, Lespagnol A, Geant A, Beaucourt S *et al.* Translationally controlled tumor protein is a target of tumor reversion. *Proc Natl Acad Sci USA* 2004; **101**: 15364–15369.
32 Lucibello M, Adanti S, Antelmi E, Dezi D, Ciafre S, Carcangiu ML *et al.* Phospho-TCTP as a therapeutic target of dihydroartemisinin for aggressive breast cancer cells. *Oncotarget* 2015; **6**: 5275–5291.
33 Seo EJ, Efferth T. Interaction of antihistaminic drugs with human translationally controlled tumor protein TCTP) as novel approach for differentiation therapy. *Oncotarget* 2016; **7**: 16818–16839.

34 Fong PC, Boss DS, Yap TA, Tutt A, Wu P, Mergui-Roelvink M *et al*. Inhibition of poly (ADP-ribose) polymerase in tumors from BRCA mutation carriers. *N Engl J Med* 2009; **361**: 123–134.
35 Woodhouse BC, Dianova II, Parsons JL, Dianov GL. Poly(ADP-ribose) polymerase-1 modulates DNA repair capacity and prevents formation of DNA double strand breaks. *DNA Rep* 2008; **7**: 932–940.
36 Bryant HE, Schultz N, Thomas HD, Parker KM, Flower D, Lopez E *et al*. Specific killing of BRCA2-deficient tumours with inhibitors of poly(ADP-ribose) polymerase. *Nature* 2005; **434**: 913–917.
37 Bouwmeester T, Bauch A, Ruffner H, Angrand PO, Bergamini G, Croughton K *et al*. A physical and functional map of the human TNF-alpha/NF-kappa B signal transduction pathway. *Nat Cell Biol* 2004; **6**: 97–105.
38 Major MB, Camp ND, Berndt JD, Yi X, Goldenberg SJ, Hubbert C *et al*. Wilms tumor suppressor WTX negatively regulates WNT/beta-catenin signaling. *Science* 2007; **316**: 1043–1046.
39 Gunaratne J, Goh MX, Swa HL, Lee FY, Sanford E, Wong LM *et al*. Protein interactions of phosphatase and tensin homologue (PTEN) and its cancer-associated G20E mutant compared by using stable isotope labeling by amino acids in cell culture-based parallel affinity purification. *J Biol Chem* 2011; **286**: 18093–18103.
40 Zhang D, Li F, Weidner D, Mnjoyan ZH, Fujise K. Physical and functional interaction between myeloid cell leukemia 1 protein (MCL1) and fortilin. The potential role of MCL1 as a fortilin chaperone. *J Biol Chem* 2002; **277**: 37430–37438.
41 Cucchi U, Gianellini LM, De Ponti A, Sola F, Alzani R, Patton V *et al*. Phosphorylation of TCTP as a marker for polo-like kinase-1 activity *in vivo*. *Anticancer Res* 2010; **30**: 4973–4985.
42 Jung J, Kim M, Kim MJ, Kim J, Moon J, Lim JS *et al*. Translationally controlled tumor protein interacts with the third cytoplasmic domain of Na,K-ATPase alpha subunit and inhibits the pump activity in HeLa cells. *J Biol Chem* 2004; **279**: 49868–49875.
43 Katsogiannou M, Andrieu C, Baylot V, Baudot A, Dusetti NJ, Gayet O *et al*. The functional landscape of Hsp27 reveals new cellular processes such as DNA repair and alternative splicing and proposes novel anticancer targets. *Mol Cell Proteomics* 2014; **13**: 3585–3601.
44 Aglipay JA, Martin SA, Tawara H, Lee SW, Ouchi T. ATM activation by ionizing radiation requires BRCA1-associated BAAT1. *J Biol Chem* 2006; **281**: 9710–9718.
45 Low LH, Chow YL, Li Y, Goh CP, Putz U, Silke J *et al*. Nedd4 family interacting protein 1 (Ndfip1) is required for ubiquitination and nuclear trafficking of BRCA1-associated ATM activator 1 (BRAT1) during the DNA damage response. *J Biol Chem* 2015; **290**: 7141–7150.
46 Liu J, Yuan Y, Huan J, Shen Z. Inhibition of breast and brain cancer cell growth by BCCIPalpha, an evolutionarily conserved nuclear protein that interacts with BRCA2. *Oncogene* 2001; **20**: 336–345.
47 Baylot V, Katsogiannou M, Andrieu C, Taieb D, Acunzo J, Giusiano S *et al*. Targeting TCTP as a new therapeutic strategy in castration-resistant prostate cancer. *Mol Ther* 2012; **20**: 2244–2256.
48 Jorge RE, Acion L, Burin DI, Robinson RG. Sertraline for preventing mood disorders following traumatic brain injury: A Randomized Clinical Trial. *JAMA Psychiatry* 2016; **73**: 1041–1047.
49 Wang LF, Huang JW, Shan SY, Ding JH, Lai JB, Xu Y *et al*. Possible sertraline-induced extrapyramidal adverse effects in an adolescent. *Neuropsychiatr Dis Treat* 2016; **12**: 1127–1129.
50 Rappsilber J, Ishihama Y, Mann M. Stop and go extraction tips for matrix-assisted laser desorption/ionization, nanoelectrospray, and LC/MS sample pretreatment in proteomics. *Anal Chem* 2003; **75**: 663–670.
51 Xu H, Dephoure N, Sun H, Zhang H, Fan F, Liu J *et al*. Proteomic profiling of paclitaxel treated cells identifies a novel mechanism of drug resistance mediated by PDCD4. *J Proteome Res* 2015; **14**: 2480–2491.

Supplementary Information accompanies this paper on the Oncogene website (http://www.nature.com/onc)